LAMINAR FLAME CHARACTERISTCS OF ETHANOL-AIR MIXTURE: EXPERIMENTAL AND SIMULATION STUDY

by

Cangsu XU[a*], Anhao ZHONG[a], Yangyang HU[a], Xiaolu LI[b], Xuan ZHOU[a]

[a]College of Energy Engineering, Zhejiang University, Hangzhou 310027, China

[b]College of Mechanical and Electrical Engineering, China Jiliang University, Hangzhou 310018, China

Experimental test for laminar combustion of ethanol-air mixture was investigated in a constant volume combustion bomb (CVCB). The laminar burning velocity and Markstein length were determined over an extensive range of equivalence ratios from 0.7 to 1.6 under an initial condition of 0.1 MPa pressure and 358 K temperature, with high-speed schlieren system. The methods of linear extrapolation and nonlinear extrapolation are compared and discussed. Apart from experiments, simulation was carried out in Chemkin by using the Marinov ethanol oxidation mechanism. Results indicate that nonlinear extrapolation is more suitable to calculate the laminar burning velocity of ethanol-air mixture. The overall trends of laminar burning velocity versus equivalence ratio are consistent between the experiment and simulation. The peak values of the laminar burning velocity from present experiment and simulation are 531.2 mm/s and 565.3 mm/s, both appearing at the equivalence ratio of 1.1. Moreover, the Markstein length of ethanol-air mixtures generally decreases with increasing equivalence ratio.

Keywords: *ethanol, spherical flames, laminar burning velocity, Markstein length, simulation*

1. Introduction[1]

In recent years, in order to deal with the shortage of fossil fuels and increasingly severe pollution problems brought by extensive application of internal combustion engine, focus has been drawn towards alternative fuels. Among many alternative fuels for the internal combustion engine, including natural gas, syngas, and other biofuels, renewable biofuels such as biodiesel and bioethanol [1] are the main focus of the current research. Ethanol, generated from lignocellulose, corn, wood and other biomass, is considered to be one of the most promising alternative fuels for spark-ignition engines due to its high thermal efficiency and low emission characteristic [2]. The physical and chemical properties of ethanol are listed in tab. 1.

The laminar burning velocity is defined as the speed at which a planar, unstretched, adiabatic, premixed flame propagates relative to the static unburned gas. The laminar burning velocity is one of

* Corresponding author; e-mail: xucangsu@zju.edu.cn

the most significant parameters for any fuels, because it reflects the physicochemical property of the combustible mixture [3]. Accurate measurement of the laminar burning velocity is essential not only for validating the chemical reaction mechanism, but also for simulation of turbulent combustion, as well as for the design and optimization of internal combustion engine [4]. Over the past decades, much effort has been devoted to obtaining the accurate data of laminar burning velocity. At present, there are several experimental methods which have been used to determine the laminar burning velocity such as the Bunsen flame method [5], the heat flux method [6-9], the stagnation plane flame method [10,11], and the combustion bomb method [4,12-15]. The combustion bomb method employs spherically expanding flame to determine the laminar burning velocity. Compared to other methods, the great advantages of the combustion bomb method include the simple flame configuration and well-defined stretch rate, therefore, it is widely used for measuring laminar burning velocity, especially at high pressure [16].

Table 1. Chemical and physical properties of ethanol

Fuel property	Ethanol
Molecular formula	CH_3CH_2OH
Molecular weight (g/mol)	46.07
Boiling point (℃)	78.3
Density (g/cm^3) at 20℃	0.79
Viscosity (mPa·s) at 20℃	1.074
Heat of combustion (kJ/mol) at 25℃	1336.8
Air/Fuel ratio	8.98
Research octane number (RON)	108

Significant amounts of research on the measurement of ethanol laminar burning velocity have been done internationally. Liao *et al*. [12] have measured laminar burning velocities and Markstein lengths of ethanol-air mixtures using a constant volume combustion bomb (CVCB) at 0.1 MPa and at temperatures between 358 and 480 K, over a wide range of equivalence ratios from 0.7 to 1.4. Veloo *et al.* [11] have determined laminar burning velocities of ethanol-air mixtures in the counterflow configuration at atmospheric pressure and 343 K temperature. Konnov *et al.* [6] have used heat flux method to measure laminar burning velocities of ethanol-air flames at atmospheric pressure and temperature ranging from 298 to 358 K. Tab. 2 summarizes the recent researches of the ethanol-air laminar burning velocity measurements.

Marinov [17] has developed a detailed chemical kinetic model to successfully predict the laminar flame speed and ignition delay time of ethanol-air mixture. Based on the Marinov ethanol oxidation mechanism, Li [18] divided the whole mechanism into three parts: H_2/O_2 submechanism, C_1 submechanism and C_2 submechanism. Abianeh [19] has presented a skeletal chemical kinetic mechanism of ethanol reference fuel (including ethanol, iso-octane, n-heptane, and tolune combustion mechanisms), and the laminar flame speed of ethanol was modeled under different temperatures, pressures, and equivalence ratios.

In this study, spherically expanding flames of ethanol-air mixtures were investigated in the CVCB. Experiments were conducted at an extensive range of equivalence ratios (0.7-1.6) under an initial condition of 0.1 MPa pressure and 358 K temperature. The reason why we choose 358 K as

initial temperature is that it is beneficial for evaporation of ethanol, and we can refer to other literature values to validate the present experimental method. High-speed schlieren photography was used to record flame image sequences. Two extrapolation methods were discussed and compared. Apart from experiments, simulations were carried out in Chemkin by using a Marinov ethanol oxidation mechanism. Data from present experimental and simulation work were compared with literature data.

Table 2. Overview of the ethanol-air laminar burning velocity measurements in literature

Year	Reference	Method	p	T (K)	ϕ
2007	Liao *et al*. [12]	Bomb, linear extrapolation	0.1 MPa	358, 400,480	0.7-1.4
2009	Bradley *et al*. [13]	Bomb, linear extrapolation	0.1-1.4 MPa	300-393	0.7-1.5
2010	Veloo *et al*. [11]	Counterflow	1 atm	343	0.7-1.5
2010	Konnov *et al*. [6]	Heat flux	1 atm	298-358	0.65-1.55
2011	Lipzig *et al*. [7]	Heat flux	1 atm	298, 338	0.6-1.5
2011	Marshall *et al*.[4]	Bomb, pressure derived	50-400 kPa	310, 380, 450	0.7-1.4
2012	Varea *et al*. [14]	Bomb, nonlinear extrapolation	0.1-5 MPa	373	0.7-1.5
2013	Tran *et al*. [8]	Heat flux	6.7 kPa	333	0.7, 1.0, 1.3
2014	Dirrenberger *et al*. [9]	Heat flux	1 atm	298, 358, 398	0.8-1.6
2015	Aghsaee *et al*. [15]	Bomb, nonlinear extrapolation	1-5 bar	318, 473	0.7-1.5

2. Experimental apparatus

Fig. 1 presents the general layout of experiment apparatus, including a temperature controlled CVCB, an electrode ignition system, a sequence control system, and a high-speed Schlieren photography system [20].

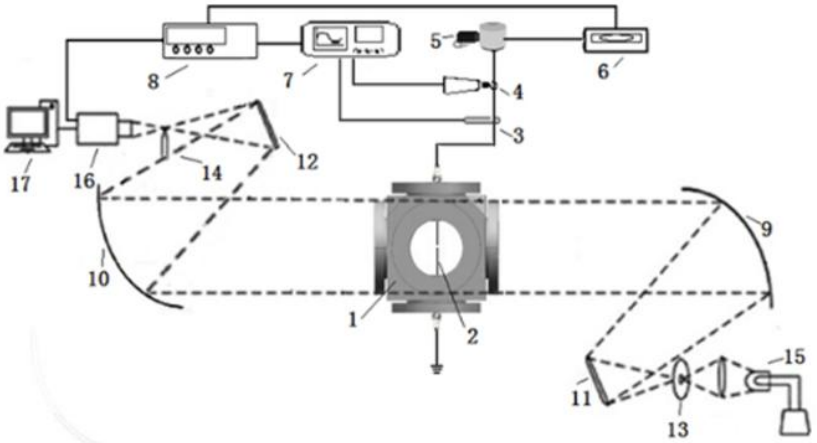

1.CVCB; 2.Central Electrodes; 3.Current Probe (Tektronix, TCP2020); 4.Coltage Probe (Tektronix, P6015A); 5.Ignition Coil; 6.Ignition Control Module; 7.Oscilloscope (Tektronix DPO2024B); 8.Digital Delay/Pulse Generator (SRS DG645); 9-10.Paraboloidal Mirror; 11-12.Flat Mirror; 13.Slit; 14.Knife Edge; 15.Xenon Lamp; 16.High-speed Camera; 17.Computer

Figure 1. Schematic diagram of experimental apparatus

2.1. CVCB

The CVCB is a cubical (200mm×200mm×200mm) chamber with a volume of 1.94 L. For optical access, three pairs of orthogonal quartz windows with diameters of 105 mm are available at six

sides of the chamber. The temperature of CVCB is controlled by six resistance heaters located in each wall and a PID controller. The pressure transducer (Kistler 6115B) combined with a charge amplifier (Kistler 5018A) is used to measure the dynamic pressure during the combustion. The maximum temperature and pressure limit of this CVCB are 600 K and 20 MPa, respectively.

2.2. Mixture preparation

Before fuel injection, the CVCB is vacuumed to approximately 50 kPa absolute pressure, and heated up to 358 K. Fuels are injected into the combustion chamber by micro syringe whose needle passes through a septum and ball-valve, in order to prevent the leakage of fuels. Then, air is introduced into the CVCB via the air inlet valve. The temperature is maintained at 358 K for at least 10 minutes to ensure the formation of homogeneous mixture.

Analytical grade ethanol used in this study is supplied by Sinopharm Chemical Raegent Company Ltd. The volume of injected fuel is calculated by the following equation:

$$V_e = \frac{p_0 V_c M_e}{\rho_e R T_0} \frac{0.21\phi}{0.21\phi + 3} \tag{1}$$

where p_0 is the initial pressure (0.1 MPa); V_c is the bomb capacity (1.94 L); M_e is the ethanol molecular weight (46.07 g/mol); ϕ is the equivalence ratio; ρ_e is the ethanol density at atmospheric temperature and pressure (0.79 g/cm^3); T_0 is the initial temperature (358 K); R is the molar gas constant (8.314 J/mol/K); the number of 3 denotes the number of moles of oxygen required for completely oxidizing one mole of ethanol.

2.3. Ignition

The ethanol-air mixture is spark-ignited using two opposite central electrodes which are made out of the spark plug. The spark is produced by high voltage in the mixture, which is characterized by a flash of light and a sharp acoustic sound. The spark releases the energy between the two opposite electrodes[20].

2.4. High-speed schlieren system

A high-speed schlieren system is employed to record the image of the flame front. A xenon lamp provides the light source, which successively passes through the focusing lens, slit, flat mirror and paraboloidal mirror to form the parallel light. The density difference between burned gas and unburned gas can be detected by parallel light, so that we can obtain the images of the flame front. Images are ultimately captured by high-speed camera (Photron FASTCAM-ultima APX) operating at 6000 fps with a resolution of 512 × 512 pixels.

2.5. Sequence control system

On account of the high requirement of temporal resolution of experiment data, we utilize a delay pulse generator (SRS DG645) to synchronously trigger the every device. When we use ignition control module to manually trigger the ignition, the module will immediately output triggering signals to delay pulse generator. At that moment, the delay time of pulse generator is zero. At the same time, the high speed camera and oscilloscope respectively receive the triggering signals and start recording

experiment data.

3. Data processing

For experimental condition, the propagation process of the ethanol-air flame front at equivalence ratio at 0.7 is shown in fig. 2(a). From these images, flame front radius can be obtained by the following equation:

$$r_f = \sqrt{\frac{S_f}{S_a}} R_0 \tag{2}$$

where S_f is the number of pixels inside the flame front, S_a is the number of pixels of the entire window, R_0 is the radius of window (52.5 mm), r_f is the flame radius. The S_f and S_a can be acquired from the quick selection tool of Photoshop CS4 software, as shown in fig. 2(b).

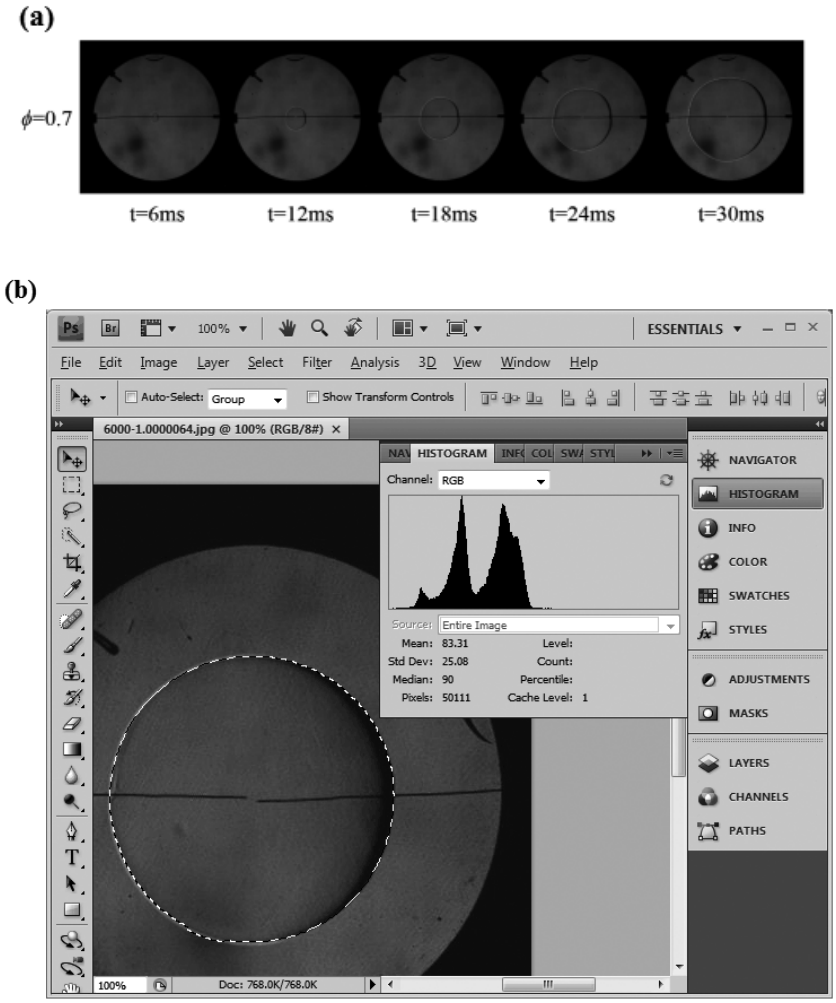

Figure 2. (a) Flame images and (b) Measurement of the number of pixels inside the flame front

Stretched laminar flame speed (S_b) is the temporal derivative of flame front radius evolution:

$$S_b = \frac{dr_f}{dt} \tag{3}$$

Fig. 3 shows stretched flame speed versus flame radius after ignition. It is seen that flame speed promoted by ignition energy is greater at the initial stage of flame propagation. Then, flame speed decreases rapidly with the consumption of ignition energy. If ignition energy is less than the minimum ignition energy of ethanol-air mixture, the flame will extinguish. If ignition energy is greater than the minimum ignition energy, flame speed after a reduction will experience a sustained increase. After the inflexion, flame propagation is promoted by chemical reaction. The flame radius of the inflexion corresponded with the ignition energy is called the critical flame radius [21]. The flame speed corresponded with the inflexion increases with ignition energy, which means the flame will reach the propagation stage more rapidly.

Flame stretch rate is defined as the Lagrangian time derivative of the logarithm of the area A of an infinitesimal element of the surface [3]. In the CVCB, during the constant pressure process, the spherical flame stretch rate (α) is uniform and can be calculated as:

$$\alpha = \frac{\mathrm{d}(\ln A)}{\mathrm{d}t} = \frac{1}{A}\frac{\mathrm{d}A}{\mathrm{d}t} = \frac{2}{r_\mathrm{f}}\frac{\mathrm{d}r_\mathrm{f}}{\mathrm{d}t} = \frac{2}{r_\mathrm{f}}S_\mathrm{b} \tag{4}$$

Fig. 4 shows stretched flame speed versus flame stretch rate. Because flame propagation at the initial stage is affected by ignition energy, at the late stage is affected by confinement and increase of pressure, only the data in the quasi-steady burning period can be used to extrapolate unstretched flame propagation speed [22]. The size range of quasi-steady burning period depends on parameters of the combustion vessel. In this work, in order to eliminate the effects as mentioned above, flame radius between 10 mm and 1.6% of total volume of the bomb is selected as the quasi-steady burning period, which corresponds to 10-19 mm.

To obtain unstretched flame speed, the effect of stretched rate to flame propagation must be removed by extrapolation methods. The most commonly used extrapolation method is the linear extrapolation method [12,13,23], which is given by the following equation:

$$S_\mathrm{b} = S_\mathrm{b}^0 - L_\mathrm{b}\alpha \tag{5}$$

where L_b is the Markstein length relative to the burned mixture, which reflects the stability of the flame [3]. In general, the theoretical basis of the linear extrapolation method demands the mixture Lewis number is near unity and the flame is weakly stretched [24].

Recently, Kelly and Law [22] gave the nonlinear model between flame speed and stretch rate. The nonlinear model is also based on low stretch rate, but allows arbitrary Lewis number, so that it can be applied for arbitrary mixture [24]. The nonlinear extrapolation method is expressed as:

$$\left(\frac{S_\mathrm{b}}{S_\mathrm{b}^0}\right)^2 \ln\left(\frac{S_\mathrm{b}}{S_\mathrm{b}^0}\right)^2 = -2\frac{L_\mathrm{b}\alpha}{S_\mathrm{b}^0} \tag{6}$$

According to the mass conservation of flame front, laminar burning velocity (u_l) can be calculated with unstretched flame propagation speed by the following equation:

$$u_\mathrm{l} = S_\mathrm{b}^0\frac{\rho_\mathrm{b}}{\rho_\mathrm{u}} \tag{7}$$

where ρ_b and ρ_u are densities of burned and unburned gases, respectively, which can be calculated from the Premixed Code of the Chemkin software.

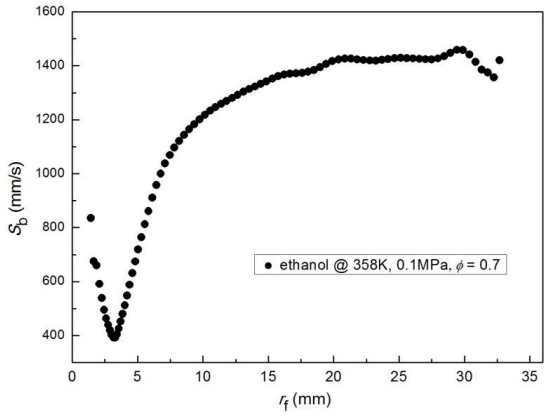

Figure 3. Flame speed versus radius in flame expansion process

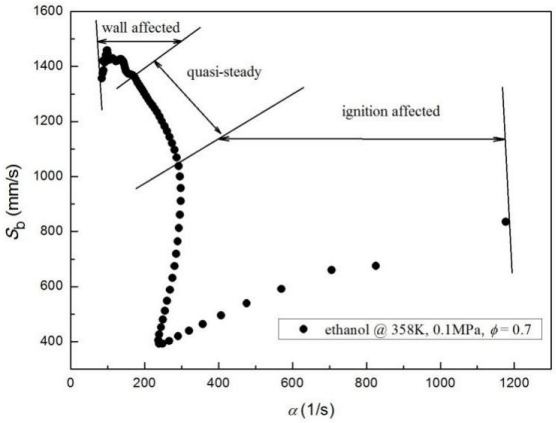

Figure 4. Flame propagation speed versus stretch rate

4. Experiment and simulation results

Fig. 5 presents the results from both linear and nonlinear extrapolation methods at the equivalence ratio of 0.7. The value of unstretched flame propagation speed from the linear extrapolation is larger than the one from the nonlinear method, which was also demonstrated by Kelley and Law [22]. From data points, it can be seen that the flame propagation speed varies a little nonlinear with stretch rate. In addition, Chen [25] has ever proposed that the linear extrapolation can only be applied to the mixture whose Lewis number is near unity, while the nonlinear extrapolation did not need to consider the range of Lewis number. At most equivalence ratio conditions, Lewis number of ethanol-air mixture is non-unity. Taking the nonlinear effect into consideration, the nonlinear extrapolation method is used throughout this study.

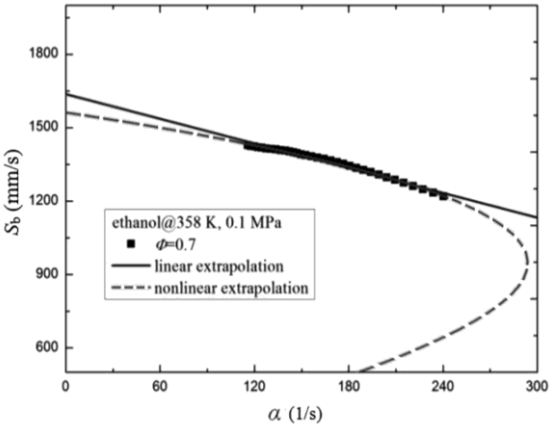

Figure 5. Comparison of the linear and the nonlinear extrapolation methods

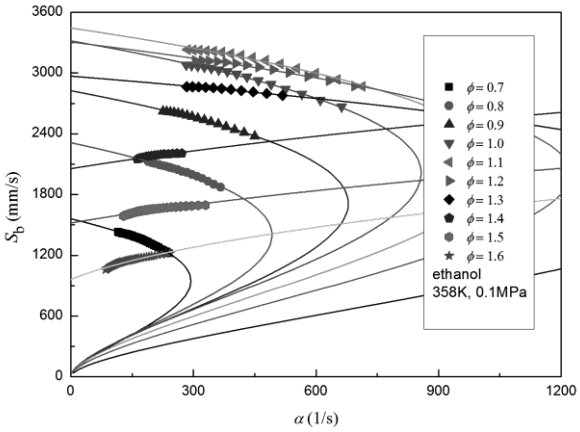

Figure 6. Nonlinear extrapolation at different equivalence ratios

Fig. 6 shows the nonlinear extrapolation progress of the experiment data at various equivalence ratios. The maximum unstretched laminar flame speed is presented at ϕ = 1.1 with a value of 3422 mm/s. When the equivalence ratio is smaller than 1.3, the Markstein length is positive, indicating that flame propagation speed decreases with the increase of stretch rate, which leads to a stable flame. On

the contrary, when the equivalence ratio is larger than 1.3, the Markstein length is negative, indicating that the flame speed increases with the increase of stretch rate. In this case, if any protuberances appear at the flame front, the flame propagation speed at the protruding position will increase, and augment the instability of the flame [3]. According to fig. 7, Markstein length shows the declining trend with the increase of equivalence ratio, and decreases more obviously for rich ethanol-air mixtures.

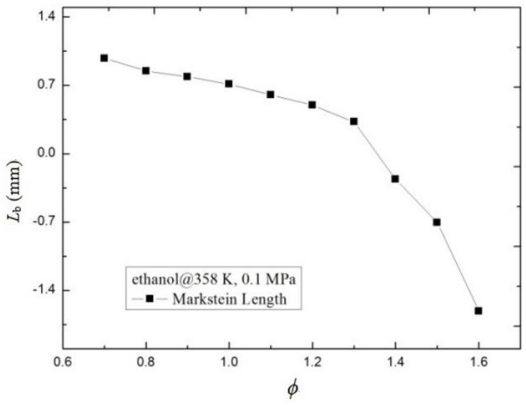

Figure 7. Markstein length L_b versus equivalence ratio

Marinov [17] has developed a detailed chemical kinetic model for ethanol oxidation, involving 56 species and 351 reversible reactions. The branching ratios for H-atom abstraction reactions, which are important for the prediction of laminar flame speed, have been estimated by using rate constants from analogous reactions that exhibit similar bond strengths as found in ethanol. In addition, rate constants for the ethanol decomposition reactions have been determined towards RRKM/Master equation calculations. Comparing the simulation results with experimental data, the validity of the Marinov oxidation mechanism has been proved by subsequent studies.

Because the Marinov ethanol oxidation mechanism is the basic theory of other mechanism, this work used Marinov mechanism to simulate laminar burning characteristics of ethanol-air mixtures in Chemkin software.

Fig. 8 shows the comparison of the laminar burning velocities from the present experiment and simulation. In addition, literature data published in recent years are also shown as references (Bradley *et al*. [13] and Liao *et al*. [12] by combustion bomb method, Dirrenberger *et al.* [9] by heat flux method, simulation data by using Li mechanism [18] and Leplat mechanism [26]). In Fig. 8, scatter points represent the experiment data, and fitting curves represent simulation results.

A global agreement is observed between the experimental data and simulation results. The model successfully predicts the effect of equivalence ratio on the laminar burning velocity. The peak values of the laminar burning velocity from present experiment and simulation are 531.2 mm/s and 565.3 mm/s, both appearing at the equivalence ratio of 1.1. But it can be seen that experimental values of laminar burning velocities by the nonlinear extrapolation method are overall lower than the numerical simulation results from the Marinov mechanism [17]. The maximum relative deviation between experiment and simulation occurs at equivalence ratio of 0.7, reaching 17.1%. For lean and stoichiometric mixtures, the relative deviation decreases with increasing equivalence ratio. The relative deviation for rich mixtures is apparently lower and reaches the minimum value (0.7%) at equivalence ratio of 1.3. Compared with Marinov mechanism, the simulation values of laminar

burning velocities from Li mechanism [18] are larger for rich mixtures and smaller for lean mixtures. Moreover, the simulation results from Leplat mechanism [26] are smaller than that from other two mechanisms, and the present experimental data is most consistent with Leplat mechanism.

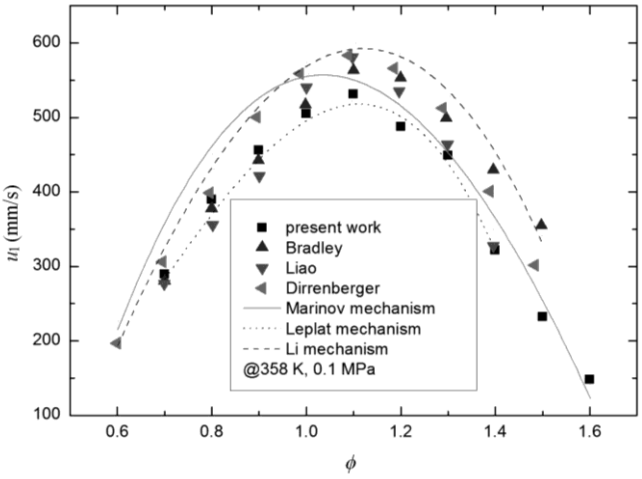

Figure 8. Comparison of the laminar burning velocities from the present experiment and simulation, and other literatures

Compared with results from combustion bomb experiment by Bradley *et al*. [13] and Liao *et al*. [12], the present experimental data of the lean ethanol-air mixtures are higher; for example, the present data is 13.4 mm/s (2.9%) higher than that from Bradley *et al*. at the equivalence ratio of 0.9. However, the experimental data of this study are considerably lower than those from Bradley *et al*. at equivalence ratios above 1.0 but are roughly equal with Liao *et al*. [12] at equivalence ratios of 1.3 and 1.4. The overall trend of laminar burning velocity versus equivalence ratio is consistent, and the maximum values all appear at equivalence ratio of 1.1. In addition, the data from Dirrenberger *et al.* [9] by heat flux method are higher than those from the experiments by combustion bomb method over a wide range of equivalence ratios, and is more consistent with Marinov mechanism [17] for lean ethanol-air mixtures.

The uncertainty of present experiment can be mostly attributed to the mixture preparation [16]. The following data of relative error in this paragraph is from the simulation. The tolerance of thermocouple (WRNK-234) is 1.5 K, and the perturbation of initial temperature can lead to an uncertainty of 1% in laminar burning velocity. The equivalence ratio can also influence the accuracy of this experiment. It is observed that for stoichiometric mixture, the relative change in laminar burning velocity is 0.5% when the equivalence ratio is changed by 0.01. However, for off-stoichiometric mixtures with equivalence ratio of 0.6 and 1.5, the relative change can reach 3.0%. The global uncertainty ΔU_{global} can be estimated by:

$$\Delta U_{global} = \sqrt{(\Delta U_{temp})^2 + (\Delta U_{equi})^2} \quad (8)$$

where ΔU_{temp} is the uncertainty caused by perturbation of initial temperature, and ΔU_{equi} is the uncertainty caused by perturbation of equivalence ratio. So the global uncertainty for this study is 1.1%-3.2%.

5. Conclusions

In this study, the spherical flame expansion processes of ethanol-air mixtures were investigated in a CVCB with the assistance of high-speed schlieren photography. Experiments were conducted at an extensive range of equivalence ratios between 0.7 and 1.6 under an initial condition of 0.1 MPa pressure and 358 K temperature. Simulation was conducted for ethanol-air premixed laminar flame in Chemkin. The main conclusions are drawn as follows:

1. Laminar burning velocity and Markstein length of ethanol-air mixtures at the initial condition of 358 K and 0.1 MPa were successfully determined by using a CVCB. Two extrapolation methods are discussed and the nonlinear extrapolation is more suitable to extract the unstreched flame propagation speed. The maximum laminar burning velocity is 531.2 mm/s at the equivalence ratio of 1.1, while the minimum value is 148.2 mm/s at the equivalence ratio of 1.6.

2. Laminar burning velocity obtained by nonlinear extrapolation method shows a similar trend with the simulation result from Marinov mechanism. For mixture of $\phi < 1.2$, the laminar burning velocity from simulation is apparently faster than that from experiment. For mixture of $\phi > 1.2$, the values of laminar burning velocity from experiment and simulation are comparatively closed. The maximum laminar burning velocity from simulation is 565.3 mm/s at the equivalence ratio of 1.1. The maximum relative deviation (17.1%) appears at the equivalence ratio of 0.7, while the minimum deviation (0.7%) occurs at the equivalence ratio of 1.3. The experimental laminar burning velocity is overall lower on average than those from simulation by Marinov mechanism, but is very consistent with the results from Leplat mechanism.

3. The Markstein lengths of ethanol-air mixtures generally decrease with the increase of the equivalence ratios, and the trend shows a sharp decrease at equivalence ratios of 1.4-1.6, where Markstein length is negative, indicating the instability of the flame. The positive value of Markstein length at the equivalence ratios below 1.3 shows that the flame propagation speed decreases with the increasing stretch rate, which means the flame is stable.

4. The global uncertainty of present experiment can be mainly attributed to the perturbation of initial temperature and equivalence ratio, and the value is 1.1%-3.2%.

Acknowledgment

This work is supported by the National Basic Research Program (No. 2013CB228106) of China, the National Natural Science Foundation of China (Nos. 50976100 and 51076138), the Public Beneficial Technology Application Research Project of Science Technology Department of Zhejiang Province (No. 2016C31102 and 2016C31112), the Fundamental Research Funds for the Central Universities (No. 2013QNA4017) of China, the Hangzhou Science Committee (No.20162013A06) of China.

Nomenclature

CVCB	- constant volume combustion bomb	A	- surface area, [mm^2]
S_b	- stretched laminar flame speed [mms^{-1}]	p_0	- initial pressure, [MPa]
S_b^0	- unstretched laminar flame speed, [mms^{-1}]	V_c	- bomb capacity, [L]
M_e	- ethanol molecular weight, [$gmol^{-1}$]	L_b	- Markstein length, [mm]
R	- molar gas constant, [$Jmol^{-1}K^{-1}$]	u_l	- laminar burning velocity, [mms^{-1}]
T_0	- initial temperature, [K]	*Greek symbols*	

S_f	- number of pixels inside the flame front	α	- stretch rate, [s^{-1}]
S_a	- number of pixels of the entire window	ϕ	- equivalence ratio
R_f	- radius of flame front, [mm]	ρ_e	- density of ethanol, [$gmol^{-1}$]
R_0	- radius of window, [mm]	ρ_b	- density of burned gas, [gL^{-1}]
t	- time, [s]	ρ_u	- density of unburned gas, [gL^{-1}]

References

[1] Zangooee Motlagh, M. R., Modarres Razavi, M. R., A Comprehensive Numerical Study of the Ethanol Blended Fuel Effect on the Performance and Pollutant Emissions in Spark-ignition Engine, *Thermal Science, 18* (2014), 1, pp. 29-38. DOI:10.2298/TSCI121005085Z

[2] Di Iorio, S., *et al.*, A Comprehensive Analysis of the Impact of Biofuels on the Performance and Emissions from Compression and Spark-Ignition Engines, *International Journal of Engine Research, 16* (2015), 5, pp. 680-690. DOI:10.1177/1468087415591924

[3] Di, Y., *et al*., Measurement of Laminar Burning Velocities and Markstein Lengths for Diethyl Ether−Air Mixtures at Different Initial Pressure and Temperature, *Energy & Fuels, 23* (2009), 5, pp. 2490-2497. DOI:10.1021/ef900015k

[4] Marshall, S. P., *et al.*, Laminar Burning Velocity Measurements of Liquid Fuels at Elevated Pressures and Temperatures with Combustion Residuals, *Combustion and Flame, 158* (2011), 10, pp. 1920-1932. DOI:10.1016/j.combustflame.2011.02.016

[5] He, Y., *et al.*, Investigation of Laminar Flame Speeds of Typical Syngas Using Laser Based Bunsen Method and Kinetic Simulation, *Fuel, 95* (2012), pp. 206-213. DOI:10.1016/j.fuel.2011.09.056

[6] Konnov, A. A., *et al.*, The Temperature Dependence of the Laminar Burning Velocity of Ethanol Flames, *Proceedings of the Combustion Institute, 33* (2011), 1, pp. 1011-1019. DOI:10.1016/j.proci.2010.06.143

[7] van Lipzig, J. P. J., *et al.*, Laminar Burning Velocities of n-Heptane, Iso-Octane, Ethanol and Their Binary and Tertiary Mixtures, *Fuel, 90* (2011), 8, pp. 2773-2781. DOI:10.1016/j.fuel.2011.04.029

[8] Tran, L., *et al.*, Experimental and Modeling Study of Premixed Laminar Flames of Ethanol and Methane, *Energy & Fuels, 27* (2013), 4, pp. 2226-2245. DOI:10.1021/ef301628x

[9] Dirrenberger, P., *et al.*, Laminar Burning Velocity of Gasolines with Addition of Ethanol, *Fuel, 115* (2014), pp. 162-169. DOI:10.1016/j.fuel.2013.07.015

[10] Egolfopoulos, F. N., *et al.*, Advances and Challenges in Laminar Flame Experiments And Implications for Combustion Chemistry, *Progress in Energy and Combustion Science, 43* (2014), pp. 36-67. DOI:10.1016/j.pecs.2014.04.004

[11] Veloo, P. S., *et al.*, A Comparative Experimental and Computational Study of Methanol, Ethanol, and n-Butanol Flames, *Combustion and Flame, 157* (2010), 10, pp. 1989-2004. DOI:10.1016/j.combustflame.2010.04.001

[12] Liao, S. Y., *et al.*, Determination of the Laminar Burning Velocities for Mixtures of Ethanol and Air at Elevated Temperatures, *Applied Thermal Engineering, 27* (2007), 2-3, pp. 374-380. DOI:10.1016/j.applthermaleng.2006.07.026

[13] Bradley, D., *et al.*, Explosion Bomb Measurements of Ethanol–Air Laminar Gaseous Flame Characteristics at Pressures up to 1.4MPa, *Combustion and Flame, 156* (2009), 7, pp. 1462-1470. DOI:10.1016/j.combustflame.2009.02.007

[14] Varea, E., *et al.*, Measurement of Laminar Burning Velocity and Markstein Length Relative to Fresh Gases Using a New Postprocessing Procedure: Application to Laminar Spherical Flames for ,Methane, Ethanol and Isooctane/Air Mixtures, *Combustion and Flame, 159* (2012), 2, pp. 577-590. DOI:10.1016/j.combustflame.2011.09.002

[15] Aghsaee, M., *et al.*, Experimental Study of the Kinetics of Ethanol Pyrolysis and Oxidation Behind Reflected Shock Waves and in Laminar Flames, *Proceedings of the Combustion Institute, 35* (2015), 1, pp. 393-400. DOI:10.1016/j.proci.2014.05.063

[16] Chen, Z., On the Accuracy of Laminar Flame Speeds Measured from Outwardly Propagating Spherical Flames: Methane/Air at Normal Temperature and Pressure, *Combustion and Flame, 162* (2015), 6, pp. 2442-2453. DOI:10.1016/j.combustflame.2015.02.012

[17] Marinov, N. M., A Detailed Chemical Kinetic Model for High Temperature Ethanol Oxidation, *International Journal of Chemical Kinetics, 31* (1999), 3, pp. 183-220

[18] Li, J., Experimental and Numerical Studies of Ethanol Chemical Kinetics, Ph. D. thesis, Princeton University, USA, 2004

[19] Abianeh, O. S., Development of a New Skeletal Chemical Kinetic Mechanism for Ethanol Reference Fuel, *Journal of Engineering for Gas Turbines and Power, 137* (2015), 6, pp. 1-9. DOI:10.1115/1.4029055

[20] Xu, C., *et al.*, A Comparative Study of Laser Ignition and Spark Ignition with Gasoline–Air Mixtures, *Optics & Laser Technology, 64* (2014), pp. 343-351. DOI:10.1016/j.optlastec.2014.05.009

[21] Chen, Z., *et al.*, On the Critical Flame Radius and Minimum Ignition Energy for Spherical Flame Initiation, *Proceedings of the Combustion Institute, 33* (2011), 1, pp. 1219-1226. DOI:10.1016/j.proci.2010.05.005

[22] Kelley, A. P., Law, C. K., Nonlinear Effects in the Extraction of Laminar Flame Speeds from Expanding Spherical Flames, *Combustion and Flame, 156* (2009), 9, pp. 1844-1851. DOI:10.1016/j.combustflame.2009.04.004

[23] Bradley, D., *et al.*, The Measurement of Laminar Burning Velocities and Markstein Numbers for Iso-octane–Air and Iso-octane–n-Heptane–Air Mixtures at Elevated Temperatures and Pressures in an Explosion Bomb, *Combustion and Flame, 115* (1998), 1–2, pp. 126-144. DOI:10.1016/S0010-2180(97)00349-0

[24] Wu, F., *et al.*, Uncertainty in Stretch Extrapolation of Laminar Flame Speed from Expanding Spherical Flames, *Proceedings of the Combustion Institute, 35* (2015), 1, pp. 663-670. DOI:10.1016/j.proci.2014.05.065

[25] Chen, Z., On the Extraction of Laminar Flame Speed and Markstein Length from Outwardly Propagating Spherical Flames, *Combustion and Flame, 158* (2011), 2, pp. 291-300. DOI:10.1016/j.combustflame.2010.09.001

[26] Leplat, N., *et al.*, Numerical and experimental study of ethanol combustion and oxidation in laminar premixed flames and in jet-stirred reactor, *Combustion and Flame, 158* (2011), 4, pp. 705-725. DOI:10.1016/j.combustflame.2010.12